Desalination and Water Treatment
www.deswater.com

doi: 10.5004/dwt.2018.22622

118 (2018) 216–229
June

Removal of heavy metals using self-integrating bio-adsorbent from agricultural by-products and marine waste materials

Norhafiza Ilyana Yatim[a], Marinah Mohd Ariffin[a,*], Sofiah Hamzah[b]

[a]*School of Marine and Environmental Sciences, Universiti Malaysia Terengganu, 21030 Kuala Nerus, Terengganu, Malaysia, Tel. +6096683130; emails: erin@umt.edu.my (M.M. Ariffin), hafiza_ilyana@yahoo.com (N.I. Yatim)*
[b]*School of Ocean Engineering, Universiti Malaysia Terengganu, 21030 Kuala Nerus, Terengganu, Malaysia, email: sofiah@umt.edu.my*

Received 10 August 2017; Accepted 16 June 2018

ABSTRACT

The potential use of agriculture and marine biowaste to produce an adsorbent for the removal of heavy metals from wastewater was studied. A bio-adsorbent was produced from the combination of rice straws and bulk seashells via self-assembled precipitation method. The chitosan:hydroxyapatite ratio in coating rice straw was set at 1:1. The molarity of the stabilizer (sodium hydroxide) was manipulated to determine the highest adsorption capacity of selected heavy metals and its effect on the physical and chemical properties of the prepared adsorbents. Isotherm tests showed that the equilibrium sorption data were better represented by the Langmuir model. The optimum bio-adsorbent (25-CH/HAP/RSA1.5M) was composed of 25% weight combination of chitosan:hydroxyapatite and stabilizer solution with a molarity of 1.5 mol L^{-1} showed the highest adsorption of heavy metal ions and was selected for subsequent study. Lead(II) (75.19) had the highest adsorption capacity of heavy metal (q_{max}), followed by zinc(II) (47.39), manganese(II) (22.73), iron(III) (19.23), nickel(II) (15.02), and copper(II) (10.72). Therefore, this study highlights the potential of an adsorbent derived from rice straw and seashells as a cost-effective alternative for heavy metal removal.

Keywords: Hydroxyapatite; Green adsorbent; Wastewater treatment; Seashell waste; Heavy metal

1. Introduction

The prevention and control of water pollution caused by heavy metals are of great emphasis. Water pollution can be caused by both natural and industrial activities. Some of the heavy metal ions are micronutrients that are needed by living organisms. However, if in excess, they may cause hyper accumulation in some plants and can be transferred to humans via ingestion can cause adverse effects. Lead may cause damage to the kidney, brain, gastrointestinal distress, and inhibit the physical and mental development of infants and children [1,2]. Copper contamination may cause toxicity to neurosystem known as Wilson's disease and damages the kidney. Overexposed to nickel may cause cancer of lungs, nose, and bone [3]. The prolonged exposure to cadmium, mercury, lead, aluminum, zinc, and arsenic may cause congenital anomaly/birth defects, and trigger cancer disease and neurological disorders [4]. The Parkinson disorder is related to the long-term exposure of manganese through direct uptake especially in drinking water [5]. The high concentration of aluminum in drinking water also increases risks of humans getting Alzheimer and Parkinson disease. For medium poisoning, adverse effect of iron may lead to vomiting and gastrointestinal bleeding. However, severe iron poisoning may cause hepatic necrosis such as anemia and liver failure (hypoglycemia and hyperammonemia) [6,7]. In Malaysia, the drinking water quality standard was set to the maximum acceptable value of heavy metal ions (i.e., lead, copper, zinc, nickel, manganese, and iron at the values of 0.01, 1.0, 3.0, 0.02, 0.1, and 0.3 mg L^{-1}, respectively) [8].

The widely used conventional techniques of heavy metals treatment from water includes membrane filtration,

* Corresponding author.

chemical precipitation, coagulation, solvent extraction, reverse osmosis, and electrochemical removal [9]. However, these methods are costly and inefficient, with incomplete removal of heavy metals and produce toxic sludge [10]. Recently studies have focused on the creation of low-cost adsorbents for the removal of heavy metals in wastewater. Adsorption technique was found to be an effective and economic method, with high adsorption capacity toward heavy metal ions [11].

Rice straw (RS) is a harvest residue, accounting for approximately 45% from the weight of rice production. It was composed of cellulose (38.3%), hemicellulose (31.6%), lignin (11.8%), and silica (18.3%) [12]. Cellulose is a linear condensation polymer consists of d-anhydroglucopyranose with the conjunction of β-1,4-glycosidic linkages, while hemicellulose was composed of several sugar units and exhibits a chain branching. However, lignin is a complex hydrocarbon, which is comprised of the aliphatic and aromatic compound and melts at temperature of 170°C and above [13]. Commonly, RS is disposed by open burning activities. However, this activity causes air pollution in the form of volatile organic carbons, carbon monoxide, and polyaromatic hydrocarbons, all of which are potentially harmful to humans if exposed [14].

Most of the naturally available adsorbents have low metal removal and slow reaction kinetics [15]. These limitations can be alleviated if the RS is either chemically reacted or grafted onto natural polymers such as chitosan and hydroxyapatite ($Ca_{10}(PO_4)_6(OH)_2$, HAP). HAP is known as calcium phosphate ceramic or bioceramic, whose structure and composition are similar to the mineral phase of bones and teeth. About 63,000 metric ton of shell fish wastes are produced annually worldwide and about 70% of the total weight is made up of clam shells. Modification of these abundantly available residues into value-added HAP can be highly useful [16]. HAP is known to exhibit various surface characteristics, including acidity and basicity, surface charge, hydrophilicity, and porosity. The heavy metal adsorption by HAP occurs via ionic exchange reaction, surface complexation with phosphate, calcium, and hydroxyl groups and/or coprecipitation of new partially soluble phases [17]. Chitosan has also been used as a surface modification agent impregnated onto supporting surfaces as adsorption sites because its amine functional groups have strong bonding ability to various heavy metal ions [18]. HAP has also been reported as a binding material to cultivate the mechanical properties of chitosan nanofibers as well as to increase metal ions sorption efficiency [19]. Chitosan is a copolymer of 2-glucosamine and *N*-acetyl-2-glucosamine units, wherein the former constitutes a major fraction of the biopolymer chain. The adsorption characteristics of chitosan are due to the large number of hydroxyl (–OH) and primary amine ($–NH_2$) groups that act as highly active adsorption sites for metal adsorption. However, the application of chitosan has been restricted due to its inherent water sensitivity, poor thermal stability, high cost, dissolution in highly acidic solution, low surface area, and relatively low stiffness and strength, especially in moist environments [20].

Chemical modification using organic compounds, minerals, organic acids or bases, and oxidizing agents can alter the chemical properties of raw material surfaces and enhance their adsorption capacity [21–23]. Thus, there is high potential to produce bio-adsorbent in large scale using agriculture and marine biowaste since they are free and abundant in nature. The use of chitosan and HAP to modify the surfaces of RS to enhance their affinity to heavy metal is not widely explored. This combination is an attractive one because both HAP and RS are low-cost and abundantly available natural materials. The modified RS-chitosan-HAP bio-adsorbent exhibits the combination advantages of having a porous network (RS), high chemical affinity (chitosan), and superior surface characteristics (HAP), resulting in the increase of the heavy metal uptake efficiency.

Therefore, in this study, a potential bio-adsorbent that can be applied in heavy metal removal was produced from agriculture (RS) and marine (HAP) biowaste. The HAP was self-assembled with chitosan and modified RS to fabricate a new bio-adsorbent with an effective adsorption capacity. The performance of produced bio-adsorbent to remove heavy metal ions such as Zn(II), Pb(II), Cu(II), Fe(III), Ni(II), and Mn(II) was evaluated. By utilizing HAP from seashell (SS) wastes and polysaccharides from RS incorporate with chitosan for the purposes of heavy metals water treatment, two existing problems can be addressed: pollution remediation and the revalorization of existing waste materials into new value-added product.

2. Materials and methods

2.1. Materials

Glacial acetic acid (CH_3COOH, 100%) and NaOH pellets (NaOH ≥ 99.0%) were supplied by Merck (Darmstadt, Germany). Iron(III) nitrate nanohydrate ($Fe(NO_3)_3{\cdot}9H_2O$, +98%) was purchased from Acros Organics (New Jersey, USA). Lead(II) nitrate ($Pb(NO_3)_2$, ≥ 99.0%), copper(II) chloride dehydrate ($Cu(Cl)_2{\cdot}2H_2O$ ≥ 99.0%), chitosan medium molecular weight, poly-(d-glucosamine), and ammonium phosphate dibasic, ($(NH_4){\cdot}2HPO_4$ ≥ 98.0) were obtained from Sigma-Aldrich (Missouri, USA). Stock standard solution and working standard solutions were freshly prepared and stored in refrigerator prior to use. Deionized water was purified using Purelab Ultra, ELGA with millipore 18.2 μΩ. All reagents used were analytical reagent grade.

2.2. Synthesis of adsorbent

2.2.1. Alkaline rice straw

RS was collected during harvest from the paddy fields in Besut Schemes, Terengganu, Malaysia (GPS coordinates: N5.672186, E102.504262). The used RS (*Oryza sativa L.* variety MR 127) was derived from Malaysian Agricultural Research and Development Institute (MARDI) [24]. RS was cleaned with distilled water and dried in oven at 60°C for 24 h. Dried RS was grounded into powder and passed through a sieve of <212 μm pore size. Then, RS was treated with alkaline solution by adding 300 g of RS into 1,000 mL of 0.1 mol L^{-1} NaOH and mixed with an orbital shaker at 150 rpm for 1 h. The treated alkaline rice straw (RSA) was then filtered and washed to neutral pH and dried in oven at 50°C for 48 h before being stored in air tight container for further experiment.

2.2.2. Synthesis of HAP

Bulk SS were randomly collected from Teluk Ketapang beach, Terengganu, Malaysia (GPS coordinate: N5.382679, E103.116478). The SS were cleaned using tap water and dried in oven at 60°C overnight. The dried SS were crushed and pulverized before being calcinated in furnace at 1,000°C for 1 h. HAP was synthesized by mixing 150 mL solution of diammonium hydrogen phosphate to the 150 mL solution of calcined SS (CaO) with mole ratio of Ca/P = 1.68. The mixture solution was stirred at room temperature for 48 h. The white precipitate of HAP powder was filtered and washed several times with distilled water to neutralize the adsorbent. The filtered HAP was dried in oven at 100°C for 24 h, sieved (in range of 25–38 μm) and stored in dry place prior to use [25].

2.2.3. Preparation of bio-adsorbents

Bio-adsorbent of 5%-chitosan/HAP (CH/HAP; 1:1) was prepared by mixing 0.075 g of HAP powder with the dissolved chitosan (0.075 g) in acetic acid solution (100 mL, 2%). This solution was mixed in orbital shaker with a constant speed of 150 rpm at room temperature for 24 h. Then, RSA (3 g) was added and continuously stirred for another 24 h. The stabilizing agent, NaOH solution (100 mL, 0.1 mol L^{-1}) was added and the solution was stirred for 24 h. Then, additional 50 mL of NaOH (0.1 mol L^{-1}) was added and left for 1 h. Next, the supernatant was discarded using centrifuge at 3,000 rpm for 5 min, and repeated with washing the bio-adsorbent using distilled water for several times to remove any residuals. Then the bio-adsorbent was collected and dried in oven at 50°C for 48 h prior to further use. These experimental procedures were repeated to produce various formulation of bio-adsorbent by replacing the weight of CH and HAP, respectively, 15%-CH/HAP (0.225 g), 25%-CH/HAP (0.375 g), 35%-CH/HAP (0.525 g), and 45%-CH/HAP (0.675 g). The adsorbents produced were named 5-CH/HAP/RSA, 15-CH/HAP/RSA, 25-CH/HAP/RSA, 35-CH/HAP/RSA, and 45-CH/HAP/RSA, correspondingly.

To study the effect of stabilizing agent's molarities, the selected adsorbent formulation 25-CH/HAP/RSA was repeatedly produced using different stabilizing agents, NaOH solution molarities (0.5, 1.0, 1.5, and 2.0 mol L^{-1}) and named 25-CH/HAP/RSA0.5, 25-CH/HAP/RSA1.0, 25-CH/HAP/RSA1.5, and 25-CH/HAP/RSA2.0.

2.3. Instrumentation

Fourier transform infrared (FTIR) spectroscopy technique by Perkin Elmer Spectrum 2000 FTIR Spectrometer was used to identify the functional groups on bio-adsorbent using potassium bromide (KBr) pellet method and recorded in the range of 400–4,000 cm^{-1}. The morphological characteristics of the prepared adsorbents were also determined using a scanning electron microscope (JEOL model JSM-6360 LA). Thin layers of adsorbent were coated using gold (Au) to produce fine images depicting the adsorbent surfaces at high magnification and protects the surface from the electron beam with kinetic energies of about 1–25 kV. For Brunauer, Emmett, and Teller (BET) analysis, the surface area analysis was performed by using the Micromeritics, ASAP-2020 from Florida, USA. Inductively coupled plasma-optical emission spectroscopy (ICP-OES) Shimadzu was used to evaluate the concentration of heavy metal ions.

2.4. Batch adsorption studies

The bio-adsorbents prepared were further evaluated for its metal adsorption capacities through batch equilibrium studies. Multimetal ions of Fe(III), Pb(II), and Cu(II) were selected based on their common toxicity in environment. To study the effect of CH/HAP-coated RS on multimetal ions adsorption, 0.4 g of the prepared adsorbent was added into a 200 mL of 25 mg L^{-1} multimetal ions solution. The mixtures were then mixed at 150 rpm in an orbital shaker. The effect of contact time was evaluated at interval times of 15, 30, 60, 90, 120, 150, 180, 210, and 240 min and 10 mL of solution was removed and analyzed at each time interval. The concentration of metal ions was analyzed using ICP-OES. All experiments were done in triplicates. This procedure was also repeated to study the effect of stabilizing agent's molarity on heavy metals adsorption. The removal efficiency, $R\%$ and quantity of heavy metal ions adsorbed by bio-adsorbents were calculated using Eqs. (1) and (2) as follows [26]:

$$R\% = \frac{\left(C_o - C_e\right)}{C_o} \times 100\% \tag{1}$$

$$q_t = \frac{\left(C_o - C_t\right)V}{m} \tag{2}$$

where C_O, C_t, and C_e (mg L^{-1}) are the concentrations of heavy metal ions in solution at initial, at interval time t (min), and equilibrium, respectively. q_t (mg g^{-1}) is the amount of heavy metal ions adsorbed per unit mass of adsorbent at time t (min); V (L) is the total volume of heavy metal solution; and m (g) is the weight of adsorbent used.

2.5. Adsorption kinetic study

For kinetic study, optimum adsorbent was determined using different initial concentration (50–300 mg L^{-1}). 0.4 g of 25-CH/HAP/RSA1.5 was added into a 250 mL of Schott bottle containing 200 mL of heavy metal solutions, Pb(II), Fe(III), and Cu(II) of 50–300 mg L^{-1}, separately. 10 mL of the supernatant was collected using syringe filter at interval times of 15, 30, 60, 90, 120, 150, 180, 210, and 240 min for each concentration of each heavy metal ions. All experiments were carried out in triplicates. The filtered supernatant was kept in the refrigerator at 4°C before being subjected to ICP-OES analysis.

2.5.1. Pseudo-first-order kinetic model

Kinetic study is necessary to describe the biosorption mechanism of heavy metals and its potential rate-controlling steps such as mass transport and chemical reaction processes. It can be determined by fitting the experiment data to pseudo-first-order and pseudo-second-order kinetic models.

The linear equation of pseudo-first-order is expressed in Eq. (3) as follows [27]:

$$\log\left(q_e - q_t\right) = \log q_e - \frac{K_1 t}{2.303} \tag{3}$$

where q_e and q_t (mg g^{-1}) are the amount of adsorbate adsorbed in equilibrium and at time, t (min), respectively. A linear graph was plotted using equation log ($q_e - q_t$) versus t where K_1 is the rate constant of pseudo-first-order adsorption.

2.5.2. Pseudo-second-order model

The linear equation of pseudo-second-order may be represented by Eq. (4) as follows [28,29]:

$$\frac{t}{q_t} = \frac{1}{K_2 q_e^2} + \frac{1}{q_e} t \tag{4}$$

A linear graph of pseudo-second-order was plotted using the equation t/q_t versus t, where $K_2 q_e^2$ is the initial biosorption rate (mg g^{-1} min^{-1}) or known as h, and K_2 is the rate constant of pseudo-second-order kinetics (g mg^{-1} min^{-1}).

2.6. Equilibrium adsorption isotherm

The adsorption isotherm was determined by adding 0.4 g of 25-CH/HAP/RSA1.5 in 200 mL of Pb(II), Fe(III), and Cu(II) respectively, each with a concentration of 50 mg L^{-1}. After reaching equilibrium, 10 mL of the supernatant was taken out using syringe and filtered with Whatman cartridge filter, nylon (0.45 μm) at interval times of 15, 30, 60, 90, 120, 150, 180, 210, and 240 min for each heavy metal ions. All experiments were carried out in triplicates.

The filtered supernatant was kept in the refrigerator at 4°C prior to ICP-OES analysis to determine the concentration of the heavy metal solutions. All experiments were carried out in triplicates.

2.6.1. Freundlich isotherm equation

The Freundlich isotherm model represents a nonideal sorption on heterogeneous surfaces and multilayer sorption [30]. Relationship between the adsorbent surface and adsorbate in equilibrium state is expressed by the plotted adsorption isotherms. The Freundlich isotherm is represented as follows [31]:

$$\log q_e = \log k_F + \frac{1}{n} \log C_e \tag{5}$$

where k_F and $1/n$ are the Freundlich constants (mg g^{-1}) related to the biosorption capacity and biosorption intensity (dimensionless) of the adsorbent, respectively. Both Freundlich constants can be obtained directly from the intercept and slope of the linear plot log q_e against log C_e, respectively.

2.6.2. Langmuir isotherm equation

The monolayer adsorption can be explained by the Langmuir isotherm. The Langmuir equation can be written as follows [32]:

$$\frac{C_e}{q_e} = \frac{1}{q_m k_L} + \frac{C_e}{q_m} \tag{6}$$

where q_e is the amount of adsorbate adsorbed at equilibrium (mg g^{-1}), k_L is the Langmuir constant related to net enthalpy (L mg^{-1}), q_m is the maximum sorption capacity corresponding to the complete monolayer coverage (mg g^{-1}), and C_e is the equilibrium solute concentration (mg L^{-1}). The value of k_L and q_m are obtained from the intercept and slope of the linear plot of C_e/q_e over C_e, respectively.

2.7. Real sample analysis

For real sample analysis, the adsorption system was done in a 2 g L^{-1} system. 50 mL of samples (WW-1,WWS-2, WW-3, WW-4, and WW-5) were poured into 50 mL of centrifuge tubes, respectively, and then 0.1 g of 25%CH-HAP48/RSA1.5M was added into the samples. These mixtures were shaken in an orbital shaker at 150 rpm for 240 min and then separated via centrifuge at 3,000 rpm for 5 min before storing in the refrigerator at 4°C prior to ICP analysis to validate the existence of heavy metal ions. pH was measured using a portable pH meter before and after adsorption. All experiments were done in triplicates. Table 1 summarizes the location and type of wastewater sampling that was conducted.

3. Result and discussion

3.1. Selection of optimum bio-adsorbent

Fig. 1 displays the surface of RS coated with different formulation of CH/HAP with the ratio of 1:1. The deposited CH/HAP molecules on the RSA surfaces were in the form of oval beads. The nucleation and growth of CH/HAP molecules resulted in the formation of bulky agglomerates in various sizes randomly deposited on the RSA surface.

In addition, the CH/HAP (1:1) formulation affected the chemical properties of the adsorbent (Fig. 2). Different formulation (%) of CH/HAP resulted in different adsorbing capability of the selected heavy metal ions, that is, Fe(III), Pb(II), Cu(II), Ni(II), Mn(II), and Zn(II).

Based on the slope at the first 60 min, 25%-CH/HAP showed highest heavy metal ions adsorbing capability, followed by 15%-CH/HAP > 45%-CH/HAP > 35%-CH/HAP > 5%-CH/HAP. These prepared bio-adsorbents showed higher affinity toward heavy metal ions Fe(III) followed by Pb(II), Cu(II), Ni(II), Mn(II), and Zn(II). The availability of functional groups hydroxyl, OH (in HAP) and amine, NH_2 (in chitosan) in the adsorbent enabled Fe(III) to be adsorbed,

Table 1
The detail of real wastewater samples

No	Sample ID	Type of water sample
1	WW-1	River near to the construction site
2	WW-2	Recreational lake
3	WW-3	Sewage from factory site
4	WW-4	Batik discharge
5	WW-5	Control (deionized water)

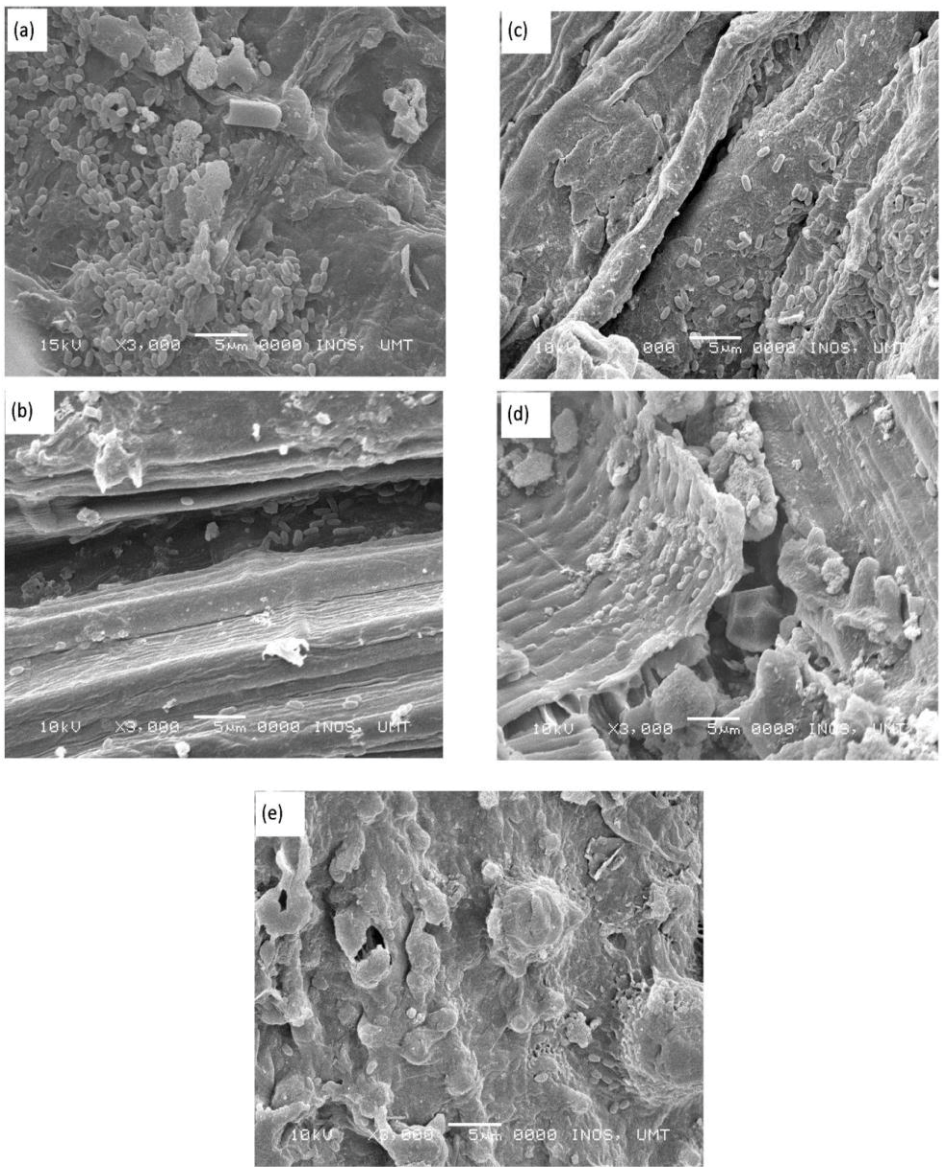

Fig. 1. SEM micrograph at 3,000 magnifications of prepared bio–adsorbents: (a) 5-CH/HAP/RSA, (b) 15-CH/HAP/RSA, (c) 25-CH/HAP/RSA, (d) 35-CH/HAP/RSA, and (e) 45-CH/HAP/RSA.

and the higher oxidation number of 3+ in Fe(III) made it the most preferable [33]. The higher atomic number and ionic radius of Pb(II) ions contributed to its higher adsorption compared with Cu(II), Ni(II), Mn(II), and Zn(II). This finding is also similar to previous study [34]. Therefore, the formulation of 25-CH/HAP/RSA adsorbent was selected for the study on the effect of stabilizing agent's (NaOH) molarity (0.5, 1.0, 1.5, and 2.0 mol L^{-1}) on the performance of heavy metal ions adsorption. From Fig. 3, most of the metals adsorption was improved.

The bio-adsorbent 25-CH/HAP/RSA stabilized with 1.5 mol L^{-1} of NaOH showed the highest heavy metal ions adsorption (steepest slopes for most of the heavy metal ions analyzed). Fe(III) heavy metal ion had the highest adsorption capacity (11.88 mg g^{-1}), with the shortest equilibrium time of 30 min achieved by 25%-CH/HAP treated with 1.5 mol L^{-1}, followed by 0.1 mol L^{-1} (60 min; 10.66 mg g^{-1}), 0.5 mol L^{-1} (60 min; 10.58 mg g^{-1}), 2.0 mol L^{-1} (60 min; 11.58 mg g^{-1}), and 1.0 mol L^{-1} (120 min; 11.58 mg g^{-1}). The low adsorption capacity of other heavy metal ions might be due to the competing effect of multimetal ions of interest for sorption sites. The properties of the respective heavy metal ions and the sorbate influence their binding strength with the sorption sites. In this situation, according to the hard soft acid–base theory, hard acids tend to form complexes with hard bases and vice versa [35]. This theory was evident in this finding, with the presence of hydroxyl and phosphate groups of hard ligands contributed to the highest affinity of Fe(III) followed by Pb(II), Cu(II), Ni(II), Zn(II), and Mn(II) as shown in Fig. 4. Binding process of different metal ions on bio-adsorbent materials also depends on its properties. In principle, metal ion with larger electronegativity and lesser

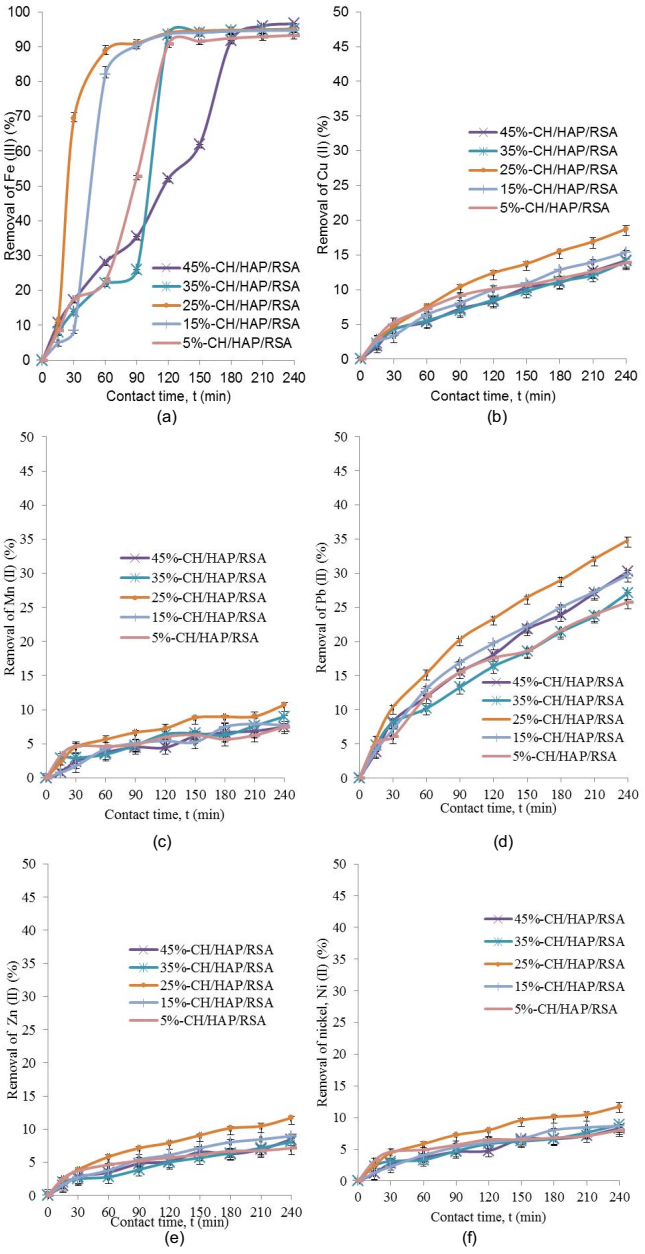

Fig. 2. Effect of adsorption capacity of various formulation of prepared bio-adsorbent for selected heavy metal ions: (a) Iron, Fe(III), (b) copper, Cu(II), (c) manganese, Mn(II), (d) lead, Pb(II), (e) zinc, Zn(II), and (f) nickel, Ni(II) (adsorbent dose: 0.4 g, multi-metal solution: 25 mg L^{-1}, 200 mL) (error bar: standard deviation).

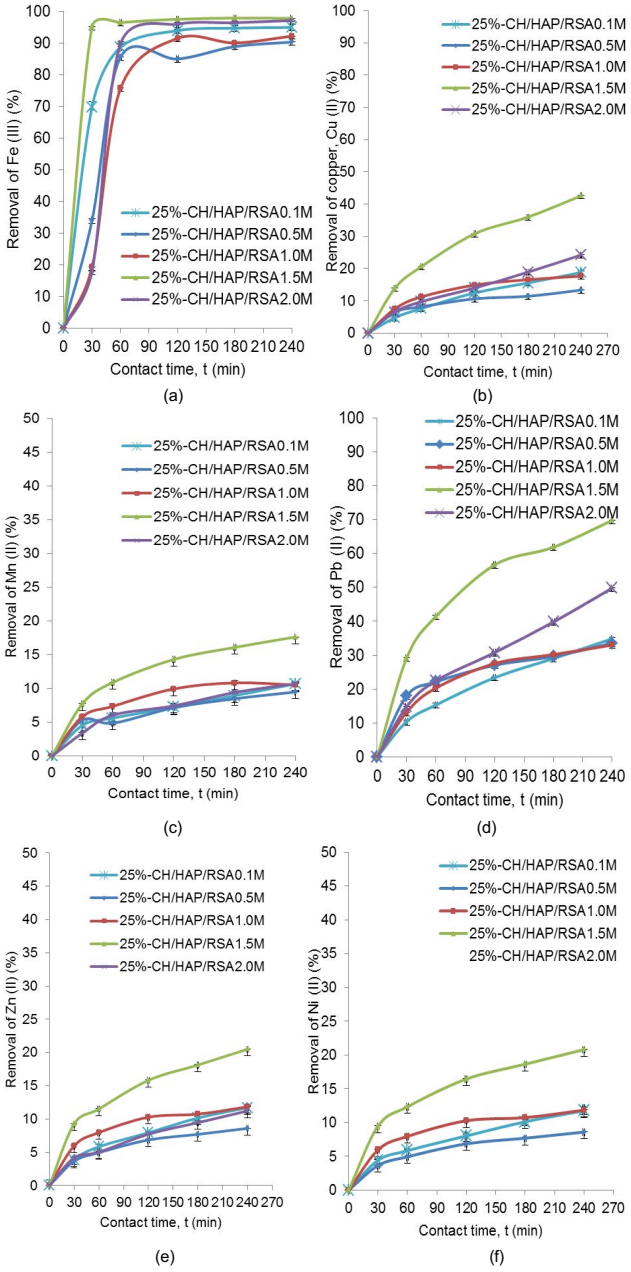

Fig. 3. Effect of adsorption capacity of optimum formulation (25%-CH/HAP/RSA) of bio-adsorbent treated with various morality of sodium hydroxide, NaOH solution for selected heavy metal ions: (a) Iron, Fe(III), (b) copper, Cu(II), (c) manganese, Mn(II), (d) lead, Pb(II), (e) zinc, Zn(II), and (f) nickel, Ni(II) (adsorbent dose: 0.4 g, multimetal solution: 25 mg L^{-1}, 200 mL) (error bar: standard deviation).

ionic radii are favorably adsorbed by the bio-adsorbent [36]. Pauling's electronegativity values for the heavy metals used in this study were: Pb (1.9), Ni (1.9), Cu (1.9) > Fe (1.8), >Zn (1.6), and Mn (1.5) [37]. For the same oxidation number, the size of cation decreases from left to right and top to bottom of a group in the periodic table [38]. In this case, the oxidation number of Fe, 3+ and the coordinate of Pb at the bottom of group contributed to their higher adsorption capacities (Fig. 4). The affinity of bio-adsorbent is affected by the ionic radius and the atomic weight of the metal ion [39].

Based on the various shapes produced from the deposited CH/HAP molecules on RSA surfaces (Fig. 5), it shows that the molarity of stabilizing agent solutions also affected the surface morphology of the prepared adsorbent.

The CH/HAP molecules were of oval beads shape when stabilized with 0.1 (Fig. 5(a)) and 1.0 mol L^{-1} (Fig. 5(c)) solution of NaOH. However, when treated with NaOH solution of molarity 0.5 (Fig. 5(b)) and 2.0 mol L^{-1}(Fig. 5(e)), the

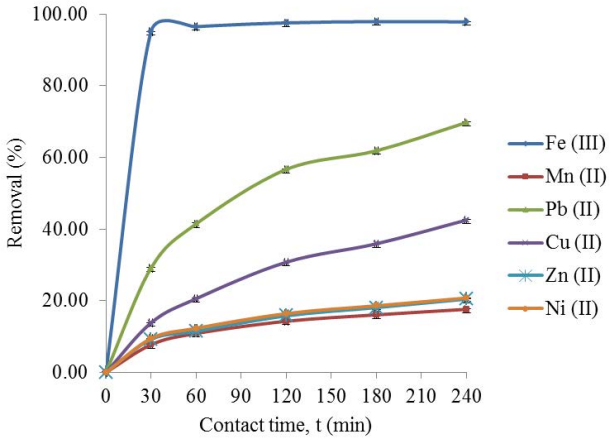

Fig. 4. Adsorption capacity of multimetal ion toward 25%-CH/HAP/RSA1.5M (adsorbent dose: 0.4 g, multimetal solution: 25 mg L^{-1}, 200 mL) (error bar: standard deviation).

CH/HAP molecules were in the form of bulky beads. This can be assumed that the nucleation and growth process of self-assembled chitosan with HAP was influenced by the surrounding pH and the matrix solution. Interestingly, the CH/HAP molecules formed needle-like structures and agglomerates when the bio-adsorbent was stabilized with 1.5 mol L^{-1} of NaOH solution (Fig. 5(d)). This needle-like molecule structures affected the adsorption capacity of heavy metal ions as shown in Fig. 3, which is exhibited the highest percentage of heavy metal ions removal. The formulation of 25%-CH/HAP was selected as optimum bio-adsorbent for subsequent study.

3.2. Characteristics of optimum bio-adsorbent

The FTIR spectrum of bio-adsorbent and its raw materials is shown in Fig. 6. FTIR spectrum of chitosan showed the presence of the adsorption peaks of amine, NH_2, and hydroxyl groups, OH which represent the polysaccharides compound. RSA spectrum showed the presence of the

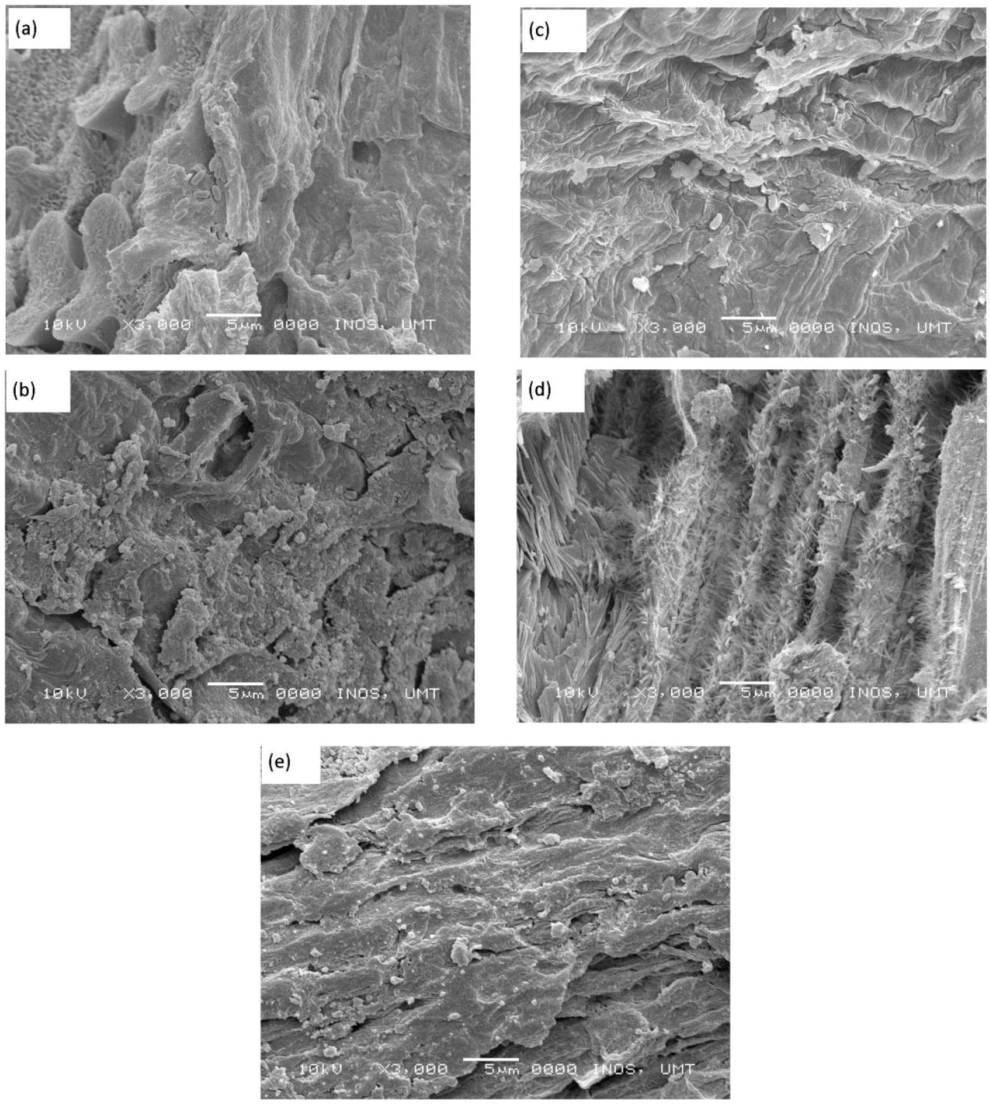

Fig. 5. SEM micrograph at 3,000 magnification of 25-CH/HAP/RSA treated with different molarity of NaOH: (a) 25-CH/HAP/RSA0.1, (b) 25-CH/HAP/RSA0.5, (c) 25-CH/HAP/RSA1.0, (d) 25-CH/HAP/RSA1.5, and (e) 25-CH/HAP/RSA2.0.

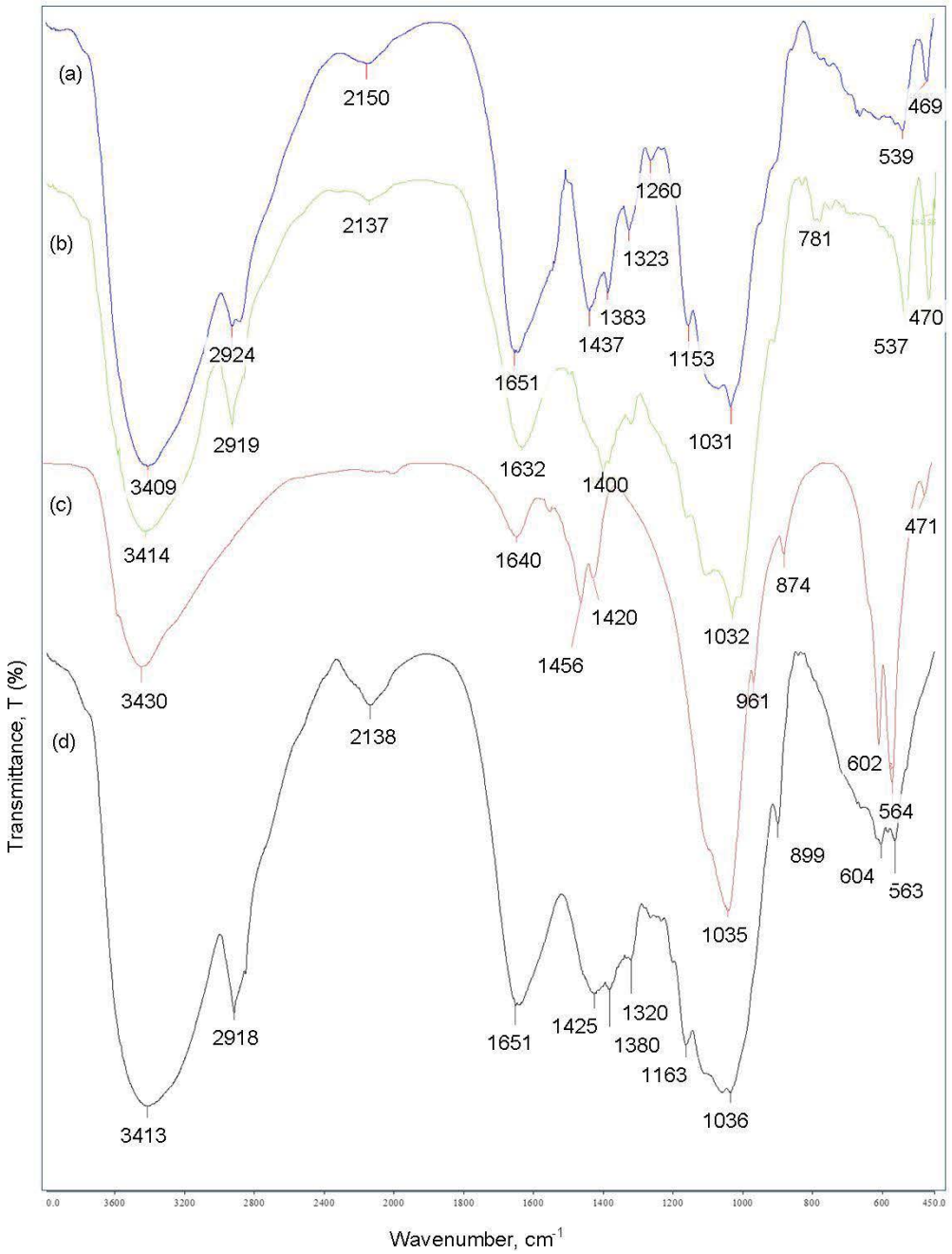

Fig. 6. The FTIR spectra of (a) chitosan (CH), (b) rice straw (RSA), (c) hydroxyapatite (HAP), and (d) 25-CH/HAP/RSA1.5.

phenolic compound and aromatic ring, C=C from the broad peak at 3,414 cm^{-1} and stretching peaks vibration at 1,632 and 1,400 cm^{-1}. Strong vibration at 1,035, 961, 602, and 564 cm^{-1} of the phosphate, PO_4^{3-} peaks were observed in the HAP spectrum. The hydroxyl group, OH was located at 3,430 cm^{-1} of the HAP spectrum. A broad peak of OH indicates that water molecules were combined with the bio-adsorbent's structure. These main functional groups found in the HAP of the current study were also reported in previous findings of prepared and commercial HAP [40,41]. Some peaks of the main characteristics of the origin materials (i.e., chitosan, RSA, and SSHAP) were found in the FTIR spectra of the optimum bio-adsorbent, 25-CH/HAP/RSA1.5. This indicates that the coating process was successful and a new adsorbent was produced. Stretching vibration (1,162, 1,035, 603, and 563 cm^{-1}) in the spectrum of 25-CH/HAP/RSA1.5 showed the overlapping of certain functional groups of chitosan (C–O; 1,153 and 1,031 cm^{-1}), SSHAP (PO_4^{3-}; 1,035 and 602–564 cm^{-1}), and RSA (Si–O; 1,032 and 537–470 cm^{-1}), indicating that new bonds were formed. The stretching peaks of C–O (1,163–1,036 cm^{-1}) in the spectrum of 25%-CH/HAP-RSA1.5 were due to the formation of hydrogen bonds between the functional groups of alkyl-substituted ether in the lignin structure of RSA and the hydroxyl group of b-1,4-glycosidic linkage in the

structure of chitosan. This similar situation was also reported in the characteristics of chitosan/lignin composite [42]. The bio-adsorbent also exhibited a stretching peak at 1,163 and 1,036 cm^{-1}, proposing that a chemical interaction occurred between C–O (1,153 and 1,031 cm^{-1}) of chitosan with the PO_4^{3-} (1,035 cm^{-1}) of HAP. The band of silica stretching of RSA disappeared as RSA overlapped with the PO_4^{3-} of HAP at 604 and 563 cm^{-1}, causing asymmetric stretching vibration. Table 2 summarizes the observed FTIR spectra band of origin materials of bio-adsorbent.

Effect of various molarities of stabilizing agent on bio-adsorbents prepared was evaluated in terms of solid surfaces characteristics using BET technique. From the isotherms graph of N_2 adsorption–desorption depicted in Fig. 7, isotherms type IV were observed in all formulations of the CH-HAP48 bio-adsorbents, implying the mesoporous structure and the hysteresis loops of a Type H3 bio-absorbent. From Table 3, the pore volumes of prepared bio-adsorbents increased as the molarity of NaOH increased. However, the NaOH molarity higher than 1.5 M showed decreasing trend. The highest value of pore volumes was achieved by 25%CH-HAP48/RSA1.5M at about 0.0272 $cm^3\ g^{-1}$. However, at the highest molarity (25%-CH-HAP48/RSA2.0M), the nature of the solid surfaces was affected, increased agglomeration of CH-HAP48, resulting in a reduced pore volume (0.0192 $cm^3\ g^{-1}$) and surface area (3.56 $m^2\ g^{-1}$) (Table 3).

3.3. Batch kinetic adsorption studies

The adsorption data of single-metal ions were fitted into pseudo-first-order and pseudo-second-order kinetics equation in Fig. 8. From the previous study, the value of R^2 close to value 1, indicates the suitability of the model with the adsorption model [43]. From the value of coefficient of determination (R^2) of both linear graphs, the adsorption data were better fitted with pseudo-second-order model. The $R^2 > 0.99$ for Zn, Pb, Cu, and Mn ions. The $R^2 > 0.9$ value for Fe(III) and Ni(II) fitted into pseudo-second-order kinetics was higher compared with R^2 of pseudo-first-order model. This model assumes that the rate of limiting step of adsorption was controlled by chemical adsorption through sharing or exchange of electrons between the adsorbate and the functional groups on the adsorbent surfaces [44]. The q_e theoretical values of the pseudo-second-order model by metal ions were similar to the q_e experimental values (Table 4). This finding is consistent with previous works on palm oil shells and carboxymethyl chitosan–hemicellulose resin as heavy metal removal from wastewater solution [45,46].

3.4. Batch equilibrium adsorption studies

The equilibrium adsorption data were fitted to Langmuir isotherm model according to the high values of R^2 for all metal ions ($R^2 > 0.9$) (Table 5). This model states that all interaction sites on the adsorbent are similar and limited in number, and each site interacts with one adsorbate only. Langmuir isotherm kinetics also suggests a homogenous and monolayer adsorption mechanism of the solute [47,48]. The equilibrium isotherm parameters obtained for the metal ions adsorption onto bio-adsorbent is presented in Table 5. The maximum adsorption capacity, q_{max} (mg g^{-1}) of heavy metal ions by bio-adsorbent was highest in Pb(II) (75.19), followed by Zn(II) (48.08), Mn(II) (22.73), Fe(III) (14.56), Ni(II) (12.77), and Cu(II) (10.72). The single-metal ions system was found to be more effective (more adsorption) compared with multi-metal (Fig. 4) due to lesser competitive effects. The bio-adsorbent used in this study managed to recover heavy metal ions of higher adsorption capacity compared with previous heavy metal removal studies using modified RS [49,50].

The plotting of adsorption isotherm system can be classified according to the initial slope of the curves. From Fig. 9, the initial curves show the adsorption isotherms of all heavy metal ions were classified as L-curve shape which postulates to Langmuir isotherms. The system defines the flatwise solute orientation and the intermolecular interaction of monofunctional ionic substances such as ion–ion interaction [51].

Pb(II), Mn(II), and Zn(II) were classified as L2 subgroup of L-curve which is explained as the rate adsorption of solute on surface directly proportional to the concentration of a solution. While for Fe(III), Ni(II), and Cu(II) was classified as L5 subgroup of L-curve which is exhibited the second plateau which postulates to complete saturation of the surface. It also represents an amount of surface may be uncovered by re-orientation of the already adsorbed solute [52].

Table 2
The description of FTIR spectra band observed in materials of bio-adsorbent

Description	Wavenumber of sample (cm^{-1})			
	Rice straw	Chitosan	Hydroxyapatite (HAP)	25%CH-HAP48/RSA1.5M
Phenolic compound, hydroxyl, –OH	3,414	3,409	3,430	3,413
–CH stretching	2,919	2,924		2,918
Amine, $–NH_2$		1,651, 1,437		1,651
$–NO_3$		1,383–1,323		1,380–1,320
Aromatic ring, C=C	1,632, 1,400			1,425
Phosphate, $–PO_4^{3-}$			1,035, 961, 602, 564	1,036, 604
C–O stretching	1,032	1,153, 1,031		1,163
Silica stretching	537, 470			563
Carbonate, $–CO_3^{2-}$			1,456–1,420	

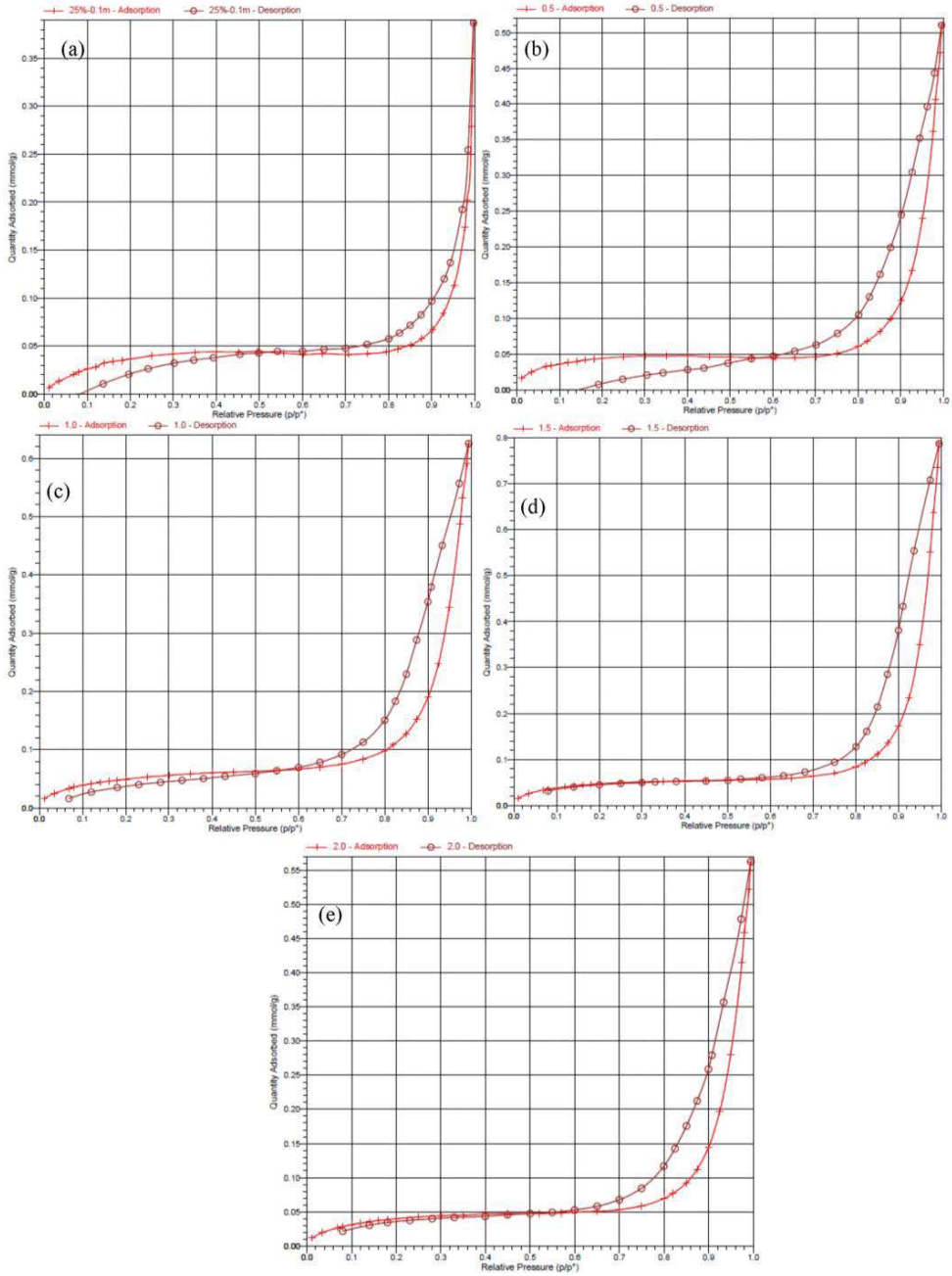

Fig. 7. The adsorption and desorption of isotherm linear plot of BET analysis of 25%-CH-HAP48/RSA adsorbent stabilized with different molarity of NaOH: (a) 0.1 M, (b) 0.5 M, (c) 1.0 M, (d) 1.5 M, and (e) 2.0 M (quantity adsorbed versus relative pressure).

Table 3
BET analysis data for 25%CH-HAP48/RSA adsorbent stabilized using various molarity of NaOH

Adsorbent	Surface area[a] ($m^2\ g^{-1}$)	Pore volume[b] ($cm^3\ g^{-1}$)	Pore width[c] (nm)
25%-CH-HAP48/RSA0.1M	3.50	0.0129	22.36
25%-CH-HAP48/RSA0.5M	3.72	0.0174	17.14
25%-CH-HAP48/RSA1.0M	4.22	0.0212	16.77
25%-CH-HAP48/RSA1.5M	4.05	0.0271	19.71
25%-CH-HAP48/RSA2.0M	3.56	0.0192	19.19

[a]BET surface area, [b]BJH desorption, [c]BJH desorption average pore width (4V/A).

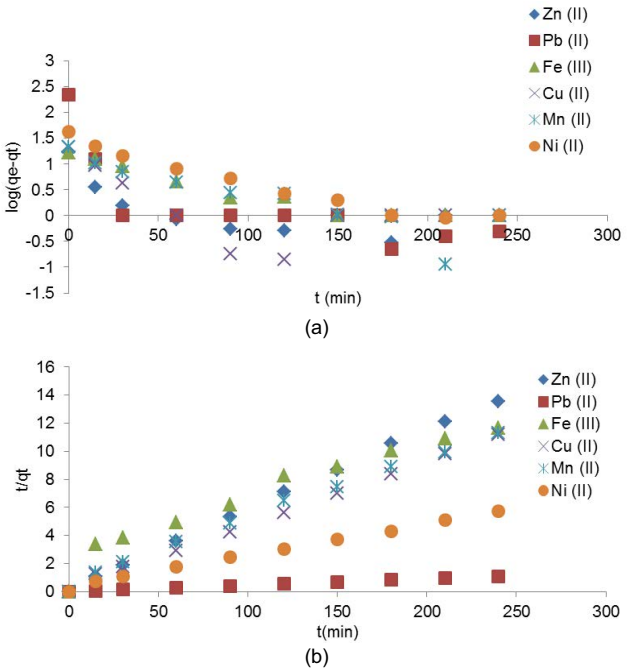

Fig. 8. Kinetic adsorption model of heavy metal ions on 25-CH/HAP/RSA1.5: (a) pseudo-first-order, and (b) pseudo-second-order.

Table 4
Kinetic parameters for Fe(III), Pb(II), Cu(II), Mn(II), Zn(II), and Ni(II) ion adsorption

Metal ion	$q_{e,exp}$	Pseudo-first-order			Pseudo-second-order		
		R^2	K_1	q_e	R^2	K_2	q_e
Fe(III)	16.85	0.892	0.0127	11.61	0.946	0.0009	22.99
Pb(II)	86.03	0.3232	0.0152	11.11	0.9952	0.0013	91.74
Cu(II)	21.44	0.2973	0.0101	4.16	0.9985	0.0079	22.08
Mn(II)	21.25	0.8033	0.0159	13.59	0.9943	0.0032	22.08
Zn(II)	54.41	0.5659	0.0177	20.14	0.9938	0.0011	61.35
Ni(II)	29.15	0.9543	0.0150	25.13	0.9827	0.0012	31.45

Table 5
Freundlich and Langmuir isotherms constants of selected heavy metal ions onto 25-CH/HAP/RSA1.5

Metal ion	Freundlich constants			Langmuir constants			
	R^2	k_F	n	R^2	q_{max}	k_L	R_L
Fe(III)	0.946	31.64	−6.64	0.9998	14.56	−1.07	−0.02
Pb(II)	0.8247	17.87	3.12	0.9988	75.19	0.17	0.12
Cu(II)	0.5923	24.22	−9.37	0.9433	10.72	−0.05	−0.75
Mn(II)	0.807	3.78	3.14	0.9877	22.73	0.04	0.37
Zn(II)	0.6019	7.14	2.63	0.9559	48.08	0.09	0.16
Ni(II)	0.0061	23.80	−22.12	0.9547	12.77	−0.04	−0.73

The binding strength of adsorbate and adsorbent was demonstrated by the k_L values, which was positively correlated with the maximum adsorption capacity of the heavy metals. Based on the R_L values, the isotherm can be either

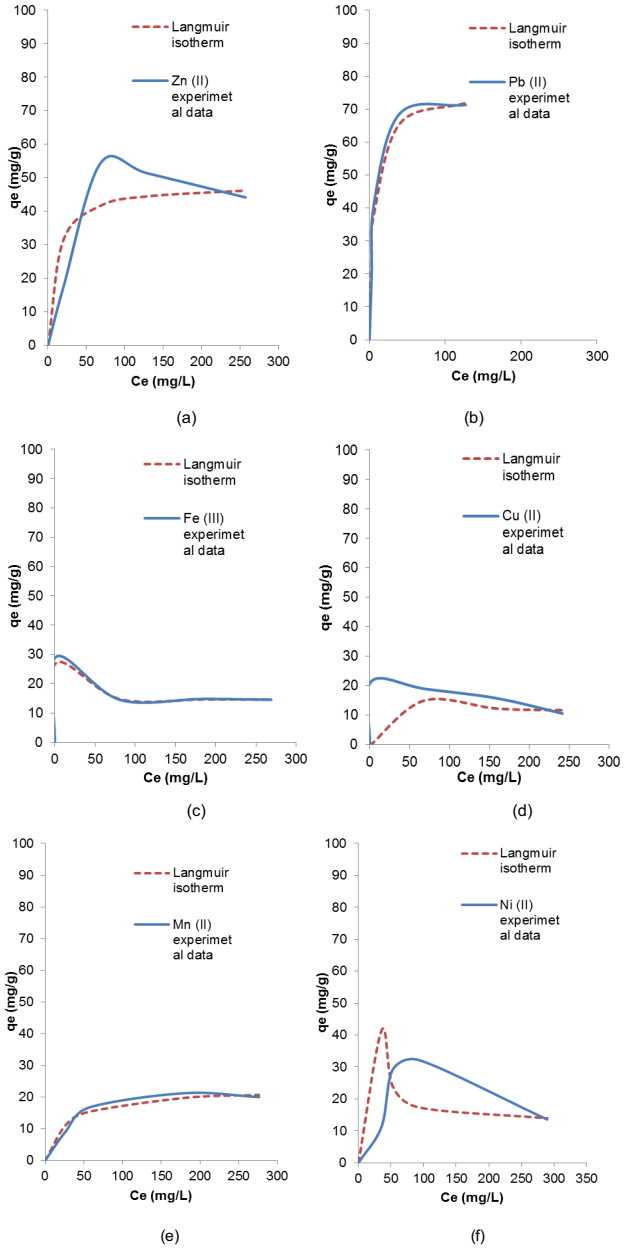

Fig. 9. Fitting of Langmuir isotherm into experimental data for heavy metal ion on 25-CH/HAP/RSA1.5: (a) Zn(II), (b) Pb(II), (c) Fe(III), (d) Cu(II), (e) Mn(II), and (f) Ni(II).

unfavorable ($R_L > 1$), linear ($R_L = 1$), or favorable ($0 < R_L$) [53]. The values of R_L were found in range 0.12–0.37 for Pb(II), Zn(II), and Mn(II) indicate it is favorable adsorption process. The negative values of Langmuir constant and R_L values for cation Fe(III), Cu(II), and Ni(II) indicate that the adsorption of these cations was difficult and unfavorable. It also highlights the inadequacy of this model to describe the adsorption process. Higher initial concentration can also decrease the adsorption capacity [54,55]. This situation was due to the reduced availability of binding sites and the external sites were occupied [56].

The heavy metal adsorption capacities for these modified RS were found to be significant with high uptake levels, thus

Table 6
The changes of pH and heavy metal ion detected in real samples before and after treatment with 25%-CH-HAP48/RSA1.5M

Sample ID	pH		Mean heavy metal concentration (mg L^{-1})													
	Before	After	Before	After	Before	After	Before	After	Before	After	Before	After	Before	After	Before	After
			Fe^{3+}		Mn^{2+}		Pb^{2+}		Cu^{2+}		Zn^{2+}		Al^{3+}		Ni^{2+}	
WW-1	2.5	7.0	14.90	0.22	0.37	0.42	0.19	0.01	0.05	0.0	0.28	0.08	7.20	0.95	0.02	0.01
WW-2	2.5	6.4	2.33	0.87	5.58	4.32	0.01	0.07	0.10	0.04	0.12	0.08	5.77	2.02	0.04	0.01
WW-3	6.0	8.8	1.19	0.67	0.04	0.01	–	–	–	–	0.21	0.03	0.08	0.02	0.01	0
WW-4	10.8	10.7	0.38	0.45	0.02	0.02	0.04	0.09	0.22	0.24	0.11	0.32	0.73	0.73	1.86	0.01
WW-5	2.1	6.3	26.03	0.08	24.19	22.48	27.83	3.39	25.65	7.27	23.83	22.06	–	–	27.83	25.35

highlighting their potential to be used as heavy metal adsorbents made from eco-friendly waste materials.

3.5. Application in real sample analysis

From the result obtained in Table 6, the pH changed from acidic to alkaline after treated with 25%CH-HAP48/RSA1.5M, indicating that interaction of metal ions with adsorbents had occurred. Samples with pH lower than 7 (samples of WW-1, WW-2, and WW-5) demonstrated high adsorption capacity due to the reduced concentration of heavy metal ions after the treatment.

The acidic pH in samples triggered the dissolution of HAP and created the partial negative charges on adsorbent surfaces, leading to heavy metal adsorption. Alkaline metal, Ca^{2+} was replaced via ionic exchange mechanism by divalent ions due to its labile characteristic [57]. In this study, the divalent ions were the heavy metal ions of Pb^{2+}, Cu^{2+}, Mn^{2+}, Zn^{2+}, and Ni^{2+}. Removal percentage of these cations tabulated displays the descending trend of removal by 25%CH-HAP48/RSA1.5M dominated by $Pb^{2+} > Cu^{2+} > Zn^{2+} > Ni^{2+} > Mn^{2+}$.

Sample WW-5 was a control sample with no interference ions. It shows high removal of Fe^{3+}, Pb^{2+}, and Cu^{2+}. Less removal of Mn^{2+}, Zn^{2+}, and Ni^{2+} can be explained through the Pearson's theory. For hard acceptors group, the adsorption was dominated by Fe^{3+} which produced $Fe(OH)_3$ yellow/brown precipitate and inhibited the interaction of Mn^{2+}. However, the intermediate group was dominated by $Pb^{2+} > Cu^{2+} > Ni^{2+} > Zn^{2+}$ ions based on their electronegativity gradient. Self-dissociation reaction of metal in water also could increase the pH of sample solution [58].

Sample pH solution close to neutral (WW-3) revealed the condition of heavy metal ion removal for cations Mn^{2+}, Zn^{2+}, Al^{3+}, and Ni^{2+}. This finding conforms with the findings of previous study, suggesting that the maximum adsorption of Zn^{2+}, Ni^{2+}, and Mn^{2+} were about pH 7.5, while for Fe^{3+}, Cu^{2+}, and Pb^{2+} occurred at pH 6.5 [59]. Different pH binding profiles for different metal ions are also postulated based on the physicochemistry interaction between the bio-adsorbent surfaces.

At pH 10, active sites from electron-pairs of biomass such as $–NO^{2+}$, –P–OH, and –Ca–OH are likely increased and thus increasing the metal ion interaction by complexation or chelating mechanism [60]. Previous study proposed that the mechanism of interchange ion was occurred between the Ni^{2+} ion and bio-adsorbent surface [61]. Therefore, the pH of the solution (WW-4) decreased after the uptake of Ni^{2+} onto the adsorbent due to the ionic exchange mechanism occurred between Ni^{2+} and H^+ in the solution. However, the slight difference in pH values was due to the low concentration of Ni^{2+} in the sample WW-4.

The result was comparable with that of previous study, suggesting that the characteristic of heavy metal ions, the pH, and the dosage of heavy metal ions influenced the adsorption capacity. However, the combination of CH, HAP, and RS strengthened each other and enhanced the performance of adsorbent in wide ranges of heavy metal ions species. In addition, the heavy metal wastewater treatment (pH near to neutral and alkaline) shows that the treated water can be returned to the environment without any additional pH adjustment. Therefore, this bio-adsorbent is made of natural sources which is environment-friendly and can be applied as pollutant adsorbents.

4. Conclusion

This study demonstrated the effectiveness of 25%-CH/HAP/RSA1.5M as the heavy metal removal adsorbent from synthetic wastewater. The adsorption capacity of modified adsorbent was higher compared with raw adsorbent. Thus, this work shows that RS and SSs are suitable to be used as bio-adsorbent and have the potential to be recommended as alternatives to the conventional method available for heavy metal removal. Consequently, it can generate profit, reduce disposing wastes, and tackle heavy metal pollution concurrently.

Acknowledgment

The authors thankfully acknowledge the Universiti Malaysia Terengganu for providing the facilities to conduct this research. This research did not receive any specific grant from funding agencies of the public, commercial, or not-for-profit sectors.

References

[1] M.R. Awual, M.M. Hasan, A. Shahat, Functionalized novel mesoporous adsorbent for selective lead(II) ions monitoring and removal from wastewater, Sens. Actuators, B, 203 (2014) 854–863.
[2] P.B. Tchounwou, C.G. Yedjou, A.K. Patlolla, D.J. Sutton, Heavy metals toxicity and the environment, NIH-PA, 101 (2012) 133–164.

[3] R. Padmavathi, M. Minnoli, D. Sangeetha, Removal of heavy metal ions from waste water using anion exchange polymer membranes, Int. J. Plast. Technol., 18 (2014) 88–99.
[4] M.W. Murad, J. Pereira, Malaysia: Environmental Health Issues, Encyclopedia of Environmental Health, 2011, pp. 577–594.
[5] N.H. Ab Razak, S.M. Praveena, A.Z. Aris, Z. Hashim, Drinking water studies: a review on heavy metal, application of biomarker and health risk assessment (a special focus in Malaysia), J. Epidemiol. Glob. Health, 5 (2015) 297–310.
[6] J. Albretsen, The toxicity of iron, an essential element, Vet. Med., 101 (2006) 82–90.
[7] M. Jaishankar, T. Tseten, N. Anbalagan, B.B. Mathew, K.N. Beeregowda, Toxicity, mechanism and health effects of some heavy metals, Interdiscip. Toxicol., 7 (2014) 60–72.
[8] S.D. Engineering, Drinking Water Quality Standard, Ministry of Health Malaysia, 2010, Available at: http://kmam.moh.gov.my/public-user/drinking-water-quality-standard.html [accessed January 12, 2017].
[9] R.K. Gautam, A. Mudhoo, G. Lofrano, M.C. Chattopadhyaya, Biomass-derived biosorbents for metal ions sequestration: adsorbent modification and activation methods and adsorbent regeneration, J. Environ. Chem. Eng., 2 (2014) 239–259.
[10] M.A. Barakat, New trends in removing heavy metals from industrial wastewater, Arabian J. Chem., 4 (2011) 361–377.
[11] F. Fu, Q. Wang, Removal of heavy metal ions from wastewaters: a review, J. Environ. Manage., 92 (2011) 407–418.
[12] P. Lu, Y.-L. Hsieh, Preparation and characterization of cellulose nanocrystals from rice straw, Carbohydr. Polym., 87 (2012) 564–573.
[13] S. Thomas, S.A. Paul, L.A. Pothan, B. Deepa, Natural Fibres: Structure, Properties and Applications, S. Kalia, B.S. Kaith, I. Kaur, Eds., Cellulose Fibers: Bio- and Nano-Polymer Composites, Springer Berlin Heidelberg, 2011.
[14] Y. Oladosu, M.Y. Rafii, N. Abdullah, U. Magaji, G. Hussin, A. Ramli, G. Miah, Fermentation quality and additives: a case of rice straw silage, Biomed. Res. Int., 2016 (2016) 1–14.
[15] J. He, J.P. Chen, A comprehensive review on biosorption of heavy metals by algal biomass: materials, performances, chemistry, and modeling simulation tools, Bioresour. Technol., 160 (2014) 67–78.
[16] S. Bramhe, T.N. Kim, A. Balakrishnan, M.C. Chu, Conversion from biowaste Venerupis clam shells to hydroxyapatite nanowires, Mater. Lett., 135 (2014) 195–198.
[17] I. Mobasherpour, E. Salahi, M. Pazouki, Comparative of the removal of Pb^{2+}, Cd^{2+} and Ni^{2+} by nano crystallite hydroxyapatite from aqueous solutions: adsorption isotherm study, Arabian J. Chem., 5 (2012) 439–446.
[18] Y. Zhou, B. Gao, A.R. Zimmerman, J. Fang, Y. Sun, X. Cao, Sorption of heavy metals on chitosan-modified biochars and its biological effects, Chem. Eng. J., 231 (2013) 512–518.
[19] M. Aliabadi, M. Irani, J. Ismaeili, S. Najafzadeh, Design and evaluation of chitosan/hydroxyapatite composite nanofiber membrane for the removal of heavy metal ions from aqueous solution, J. Taiwan Inst. Chem. Eng., 45 (2014) 518–526.
[20] G. Zuo, Y. Wan, L. Wang, C. Liu, F. He, H. Luo, Synthesis and characterization of laminated hydroxyapatite/chitosan nanocomposites, Mater. Lett., 64 (2010) 2126–2128.
[21] W.S. Wan Ngah, M.A.K.M. Hanafiah, Removal of heavy metal ions from wastewater by chemically modified plant wastes as adsorbents: a review, Bioresour. Technol., 99 (2008) 3935–3948.
[22] S.K.R. Yadanaparthi, D. Graybill, R. von Wandruszka, Adsorbents for the removal of arsenic, cadmium, and lead from contaminated waters, J. Hazard. Mater., 171 (2009) 1–15.
[23] G.B. Gholikandi, H.R. Sadabad, S. Karami, H. Masihi, Heavy metal ions removal from waste-activated sludge by Fered-Fenton electrochemical advanced oxidation process (EAOP) with the aim of agricultural land application, Desal. Wat. Treat., 93 (2017) 250–256.
[24] K.H. Lim, Rice Variety Mr 127, Malaysian Agricultural Research and Development Institute, 1991, Available at: http://agromedia.mardi.gov.my/magritech/tech_detail_fdcrop.php [accessed November 1, 2016].
[25] M.M. Ariffin, N.I. Yatim, S. Hamzah, Synthesis and characterization of hydroxyapatite from bulk seashells and its potential usage as lead ions adsorbent, Malaysian J. Anal. Sci., 21 (2017) 571–584.
[26] L. Cui, Y. Wang, L. Hu, L. Gao, B. Du, Q. Wei, Mechanism of Pb(II) and methylene blue adsorption onto magnetic carbonate hydroxyapatite/graphene oxide, RSC Adv., 5 (2015) 9759–9770.
[27] S. Lagergren, Zur theorie der sogenannten adsorption gelster stoffe, Kungliga Svenska Vetenskapsakademiens, Handlingar, 24 (1898) 1–39.
[28] Y.S. Ho, G. McKay, The kinetics of sorption of basic dyes from aqueous solution by sphagnum moss peat, Can. J. Chem. Eng., 76 (1998) 822–827.
[29] Y.S. Ho, Review of second-order models for adsorption systems, J. Hazard. Mater., B136 (2006) 681–689.
[30] R. Tabaraki, A. Nateghi, S. Ahmady-Asbchin, Biosorption of lead (II) ions on *Sargassum ilicifolium*: application of response surface methodology, Int. Biodeterior. Biodegrad., 93 (2014) 145–152.
[31] H. Freundlich, Of the adsorption of gases. Section II. Kinetics and energetics of gas adsorption, Trans. Faraday Soc., 28 (1932) 195–201.
[32] I. Langmuir, The sorption of gases on plane surface of glass, mica and platinum, J. Am. Chem. Soc., 40 (1918) 1361–1403.
[33] N. Ahalya, R.D. Kanamadi, T.V. Ramachandra, Biosorption of iron(III) from aqueous solutions using the husk of *Cicer arientinum*, Indian J. Chem. Technol., 13 (2006) 122–127.
[34] K. Pakshirajan, T. Swaminathan, Biosorption of lead, copper, and cadmium by *Phanerochaete chrysosporium* in ternary metal mixtures: statistical analysis of individual and interaction effects, Appl. Biochem. Biotechnol., 158 (2009) 457–469.
[35] G.M. Naja, V. Murphy, B. Volesky, Biosorption, Metals, Encyclopedia of Industrial Biotechnology, John Wiley & Sons, Inc., Hoboken, 2010, pp. 1–29.
[36] L.K. Wang, J.P. Chen, Y.-T. Hung, N.K. Shammaz, Heavy Metals in the Environment, CRC Press, Boca Raton, 2009.
[37] P.B. Kelter, M.D. Mosher, A. Scott, Chemistry: The Practical Science, vol. 10, Cengage Learning, Boston, 2008, pp. 320–322.
[38] E. Wiberg, N. Wiberg, Inorganic Chemistry, Academic Press, California, 2001, pp. 119–121.
[39] A. Kamari, S.N.M. Yusoff, F. Abdullah, W.P. Putra, Biosorptive removal of Cu(II), Ni(II) and Pb(II) ions from aqueous solutions using coconut dregs residue: adsorption and characterisation studies, J. Environ. Chem. Eng., 2 (2014) 1912–1919.
[40] A.L. Giraldo-Betancur, D.G. Espinosa-Arbelaez, A.D. Real-López, B.M. Millan-Malo, E.M. Rivera-Muñoz, E. Gutierrez-Cortez, P. Pineda-Gomez, S. Jimenez-Sandoval, M.E. Rodriguez-García, Comparison of physicochemical properties of bio and commercial hydroxyapatite, Curr. Appl. Phys., 13 (2013) 1383–1390.
[41 J.H. Shariffuddin, M.I. Jones, D.A. Patterson, Greener photocatalysts: hydroxyapatite derived from waste mussel shells for the photocatalytic degradation of a model azo dye wastewater, Chem. Eng. Res. Des., 91 (2013) 1693–1704.
[42] V. Nair, A. Panigrahy, R. Vinu, Development of novel chitosan–lignin composites for adsorption of dyes and metal ions from wastewater, Chem. Eng. J., 254 (2014) 491–502.
[43] M.N. Mahamad, M.A.A. Zaini, Z.A. Zakaria, Preparation and characterization of activated carbon from pineapple waste biomass for dye removal, Int. Biodeterior. Biodegrad., 102 (2015) 274–280.
[44] A. Aeisyah, M.H.S. Ismail, K. Lias, S. Izhar, Adsorption process of heavy metals by low-cost adsorbent: a review, Res. J. Chem. Environ., 18 (2014) 91–102.
[45] M.A. Hossain, H.H. Ngo, W.S. Guo, T.V. Nguyen, Palm oil fruit shells as biosorbent for copper removal from water and wastewater: experiments and sorption models, Bioresour. Technol., 113 (2012) 97–101.
[46] S.-P. Wu, X.-Z. Dai, J.-R. Kan, F.-D. Shilong, M.-Y. Zhu, Fabrication of carboxymethyl chitosan–hemicellulose resin for adsorptive removal of heavy metals from wastewater, Chinese Chem. Lett., 28 (2017) 625–632.

[47] P. Khare, A. Yadav, J. Ramkumar, N. Verma, Microchannel-embedded metal-carbon-polymer nanocomposite as a novel support for chitosan for efficient removal of hexavalent chromium from water under dynamic conditions, Chem. Eng. J., 293 (2016) 44–54.
[48] N. Passe-Coutrin, S. Altenor, D. Cossement, C. Jean-Marius, S. Gaspard, Comparison of parameters calculated from the BET and Freundlich isotherms obtained by nitrogen adsorption on activated carbons: a new method for calculating the specific surface area, Microporous Mesoporous Mater., 111 (2008) 517–522.
[49] W.M. Mousa, S.I. Soliman, H.A. Shier, Removal of some heavy metals from aqueous solution using rice straw, J. Appl. Sci. Res., 9 (2013) 1696–1701.
[50] S. Rungrodnimitchai, Modification of rice straw for heavy metal ion adsorbents by microwave heating, Macromol. Symp., 295 (2010) 100–106.
[51] C.H. Giles, D. Smith, A. Huitson, A general treatment and classification of the solute adsorption isotherm. I. Theoretical, J. Colloid Interface Sci., 47 (1974) 755–765.
[52] C.H. Giles, T.H. MacEwan, S.N. Nakhwa, D. Smithm, Studies in adsorption. Part XI. A system of classification of solution adsorption isotherms and its use in diagnosis of adsorption mechanisms and in measurement of specific surface areas of solids, J. Chem. Soc., (1960) 3973–3993.
[53] P. Chand, A.K. Shil, M. Sharma, Y.B. Pakade, Improved adsorption of cadmium ions from aqueous solution using chemically modified apple pomace: mechanism, kinetics, and thermodynamics, Int. Biodeterior. Biodegrad., 90 (2014) 8–16.
[54] B.A. Shah, A.V. Shah, P.M. Shah, Sorption isotherms and column separation of Cu(II) And Zn(II) using ortho substituted benzoic acid chelating resins, Arch. Appl. Sci. Res., 3 (2011) 327–341.
[55] J.C. Igwe, A.A. Abia, Equilibrium sorption isotherm studies of Cd(II), Pb(II) and Zn(II) ions detoxification from waste water using unmodified and EDTA-modified maize husk, Electron J. Biotechnol., 10 (2007) 536–548.
[56] S.K. Bozbaş, Y. Boz, Low-cost biosorbent: *Anadara inaequivalvis* shells for removal of Pb(II) and Cu(II) from aqueous solution, Process Saf. Environ. Prot., 103 (2016) 144–152.
[57] P. Chand, Y.B. Pakade, Synthesis and characterization of hydroxyapatite nanoparticles impregnated on apple pomace to enhanced adsorption of Pb(II), Cd(II), and Ni(II) ions from aqueous solution, Environ. Sci. Pollut. Res., 22 (2015) 10919–10929.
[58] M. Tsezos, Biosorption: a mechanistic approach, Adv. Biochem. Eng./Biotechnol., 141 (2014) 173–209.
[59] K. Tsekova, D. Todorova, S. Ganeva, Removal of heavy metals from industrial wastewater by free and immobilized cells of *Aspergillus niger*, Int. Biodeterior. Biodegrad., 64 (2010) 447–451.
[60] M. Arshadi, M.J. Amiri, S. Mousavi, Kinetic, equilibrium and thermodynamic investigations of Ni(II), Cd(II), Cu(II) and Co(II) adsorption on barley straw ash, Water Resour. Ind., 6 (2014) 1–17.
[61] K.A. Krishnan, K.G. Sreejalekshmi, R.S. Baiju, Nickel(II) adsorption onto biomass based activated carbon obtained from sugarcane bagasse pith, Bioresour. Technol., 102 (2011) 10239–10247.